$He^- \ ^2D$ weakly bound triply excited resonances: Interpretation of previously unexplained structures in the experimental spectrum

Nicos A. Piangos,[1,*] Yannis Komninos,[1,†] and Cleanthes A. Nicolaides[1,2,‡]
[1]*Theoretical and Physical Chemistry Institute, National Hellenic Research Foundation, 48 Vasileos Constantinou Avenue, Athens 11635, Greece*
[2]*Physics Department, National Technical University, Athens, Greece*

(Received 24 April 2002; revised manuscript received 1 July 2002; published 27 September 2002)

A He plus electron scattering experiment by Gosselin and Marmet [Phys. Rev. A **41**, 1335 (1990)] produced the previously known $He^- \ 2s2p^2 \ ^2D$ resonance at 58.283 ± 0.003 eV with a width $\Gamma = 59 \pm 4$ meV, and two new structures at 58.415 ± 0.005 and 58.48 ± 0.02 eV with $\Gamma < 2$ meV and $\Gamma = 70 \pm 20$ meV, respectively. The nature of these last two structures has since remained unexplained. Heuristic analysis of the spectrum of the triply excited states (TES) of He^- and of conditions of electron correlation and possible localization, and application of the state-specific theory (SST) for the calculation of electronic structures and properties led to the determination of three resonance states of ^2D symmetry that explain quantitatively the experimental data. The implementation of the SST involved the combination of suitable choices of optimized orbitals, of nonorthonormal configuration interaction, and of mixing of bound with scattering configurations. The first two ^2D TES contain the $2s2p^2$ configuration as a major component, but strong radial correlation results in the spatial separation of the two p spin orbitals. The third TES, computed systematically with up to 996 optimized configurations, is an *open-channel like* localized wave packet.

DOI: 10.1103/PhysRevA.66.032721 PACS number(s): 32.80.Dz, 31.25.Jf

I. INTRODUCTION

The work discussed in this paper was motivated by two factors: The first has to do with our continuing interest in exploring theoretically and computationally prototypical cases of resonance states of polyelectronic atoms. In this case, we examined the possibility that strongly mixing multiconfigurational Hartree-Fock (MCHF) components of the correlated wave function of the lowest intrashell triply excited state (TES) of the ^2D spectrum of He^- are responsible for the formation of weakly bound resonances just above this state [[1,2] and references therein]. Such predictions were published recently [3] concerning the existence of a $^2P^o$ weakly bound TES above the known intrashell $2s^2 2p$ resonance state.

The second factor was our desire to explain the results of experimental observations. Specifically, in 1990, Gosselin and Marmet [2] (GM), published measurements of ionization efficiency curves of electron impact on He, at energies in the range 58 to 59 eV. By fitting their data to theoretical line profiles, they obtained for the $He^- \ 2s2p^2 \ ^2D$ resonance its energy, $E = 58.283 \pm 0.003$ eV, and its width, $\Gamma = 59 \pm 4$ meV. In addition, they recognized the presence of a new structure just above the He $2s2p \ ^3P^0$ threshold (58.31 eV), consisting of two weak peaks at 58.415 ± 0.005 and 58.48 ± 0.02 eV, to which they assigned widths of about <2 and 70 ± 20 meV, respectively. At that time, no other experimental or theoretical results corroborated the existence of these features in the He^- spectrum. In their attempt to interpret them, they made analogies between the He $2p^2 \ ^3P$ state and the ground state of carbon and reached the tentative conclusion that the observed peaks represent He^- resonances with assignment $2p^3 \ ^4S^o$ and $^2D^o$.

In view of the GM publication and of the challenges that the field of resonances in the spectra of atomic negative ions (ANIs) offers, a few years ago we carried out a systematic analysis and computation of the $n = 2$ intrashell He^- resonances [4,5]. It was demonstrated that these peaks cannot be due to the $2p^3 \ ^4S^o$ state (which is a discrete state below the He $2p^2 \ ^3P$ state), or to any $2p^3$ He^- resonances. In fact, the results published thus far cannot provide even a hint as to the identity of the features C and D present in Figs. 1 and 2 of [2]. This statement is supported by the contents of the review of Buckman and Clark [6], where neither results nor discussion concerning these measurements are present. The uncertainty and vagueness surrounding this problem emerge not only from the papers cited above but also from the decades-old, close-coupling calculations of Ormonde *et al.* [7], where the positions of a number of He^- resonances were predicted, and from the conjectural discussion of [6,8] on possibilities for the interpretation of a number of structures in the region 57–66 eV of the He^- spectrum.

In conclusion, for more than 12 years since the GM publication [2], the features at 58.4–58.5 eV have remained a mystery. They have not been interpreted computationally by a first-principles theory nor have the measurements been falsified by new ones. So the following question, which is important to both theoretical and experimental work, was asked and resolved in the present work: Is the registered structure an artifact of the experiment or does it represent a physical situation?

Our approach to answering this question was to assume that the 58.4 eV structures are, indeed, representatives of

*Electronic address: npiang@eie.gr
†Electronic address: ykomn@eie.gr
‡Electronic address: can@eie.gr

triply excited resonance states of ^2D symmetry that are formed from low-lying excitations with respect to the strongly correlated $2s2p^2\ ^2D$ state which is the lowest ^2D TES in He^-. The syllogism leading to this assumption was based on the analysis of the electronic structure of the $2s2p^2\ ^2D$ resonance [1,4,5], and below, on the nature of the GM experiment, and on the fact that the calculations of [4,5] on the $n=2$ intrashell He^- TES as well as our unpublished work have demonstrated that another possible intrashell candidate state, the $2s2p^2\ ^2S$ resonance, cannot be formed around 58.4 eV.

In order to verify or reject this assumption, we implemented the state-specific theory of polyelectronic resonance states with real functions [[1,3,4,9–11] and references therein], and carried out detailed and systematic calculations aiming at obtaining and interpreting the lowest three ^2D TES in He^-. Indeed, apart from the previously known lowest ^2D TES just below the He $2s2p\ ^3P^0$ threshold at 58.3 eV, [[1,2], and this work], we established the existence of two more resonance states, which are just above the He $2s2p\ ^3P^o$ threshold. One is at $E=58.412$ eV with a narrow width of about 4 meV, and the other is at $E=58.466$ eV with $\Gamma=54$ meV. These results imply that the two unidentified peaks in the GM measurements can be interpreted as reflecting the existence of two $He^-\ ^2D$ triply excited resonance states. The calculation of their main features and properties is described below.

II. POSSIBILITY OF FORMATION OF WEAKLY BOUND ^2D TRIPLY EXCITED RESONANCES OF He^- JUST ABOVE THE LOWEST ^2D $n=2$ TES AT 58.3 eV

According to the state-specific approach, in the theory and computational search of resonance states of polyelectronic systems, the crucial element is the possibility of obtaining a reliable representation of the square-integrable wave function Ψ_0, regardless of the level of sophistication of the overall formalism. Considering the constraints that are imposed by the nature of such states, the calculation of Ψ_0 is achieved optimally in two phases. The first aims at the solution of appropriate MCHF equations. When the nuclear attraction on the outer electrons is strong, i.e., in cases of positive ions or even of neutral atoms, experience has shown that, in general, the choice of configurations and the corresponding convergence can be achieved without significant conceptual or numerical difficulty. Once the MCHF solution, Φ_{MCHF}, is known, the remaining part of Ψ_0 is obtainable variationally, to an accuracy that is relevant to the needs and significance of the problem.

On the other hand, when it comes to ANIs, the nuclear attraction is weakened considerably. The *ab initio* choice of the important zero-order function space and its self-consistent optimization can range from difficult to impossible. Furthermore, when going to a configuration interaction (CI) level, beyond Φ_{MCHF}, it is often expedient to use nonorthonormal basis functions in order to represent optimally different parts of electron correlation. We point out that, although the spectra of multiply excited states (MES) of ANIs throughout the Periodic Table have not yet been investigated systematically, it is safe to assume that, given the small energy differences, the density of resonances may become relatively high even at low excitation levels. This implies that results for the position and identification of states are meaningful only when they are characterized by high accuracy. This fact constitutes a stringent requirement for theories and calculations of ANI resonance states.

In our search for valid Ψ_0 that would correspond to the observed structures in the *e*-He collision experiment [2], we took as a fact that the probability of formation of the $2s2p^2\ ^2D$ resonance is large. (The problem of the existence and nature of this state was discussed again recently [1].) This probability is proportional to the amplitude $\langle I|T|^2D\rangle$, where $|I\rangle$ is the initial state and T is the effective transition operator. Therefore one should expect that configurations that mix heavily with the main $2s2p^2$ restricted HF(RHF) configuration, might constitute important components of real states further up in the excitation spectrum.

Indeed, our experience with the calculation of Ψ_0 has shown that there are strongly mixing singly and doubly excited configurations with respect to the RHF $2s2p^2$ configuration. The full calculation includes triply excited configurations as well. We then anticipate that it is mixtures of such configurations that constitute the main components of possible ^2D triply excited resonances, which, if the experimental peaks are real, ought to exist about 100–200 meV above the established $2s2p^2\ ^2D$ resonance state. Assuming for the sake of argument a symbolic single configuration picture based on the main $2s2p^2\ ^2D$ configuration, single orbital excitations possibly representing low-lying resonance states are

$$[(2s2p)\ ^{3,1}P^o p]\ ^2D \quad \text{or} \quad [2s(2pp)\ ^{1,3}D]\ ^2D \tag{1a}$$

and

$$[(2p^2)\ ^1D\, s]\ ^2D, \quad [(2p^2)\ ^3P,\ ^1D,\ ^1S\, d]\ ^2D. \tag{1b}$$

The different couplings (1a) have computational significance at the MCHF level since choosing one or the other affects the rate or even the possibility of convergence to an accurate solution.

It is also intriguing to consider the core correlated ''open-channel like'' (OCL) [1,4] wave function that is created from $2s2p^2$ by the channel coupling between the single excitation $s\leftrightarrow d$ and the *hole-filling* pair correlation $p^2\leftrightarrow sd$:

$$[\mathrm{He}(2s^2)d]\ ^2D+[\mathrm{He}(2p^2)\ ^1S\, d]\ ^2D. \tag{2}$$

The $[\mathrm{He}(2s^2)d]\ ^2D$ wave function corresponds to an open channel for decay: $He^-\ ^2D\rightarrow \mathrm{He}\ 2s^2\ ^1S+\varepsilon d$. (The d orbitals above are not the same radially.) However, as we have argued in [[1,4,9], and references therein], it is also possible for electron correlation (channel coupling) in MES to create a localized wave packet out of the scattering functions with the same OCL configurational character, as it sometimes happens with simple configurations representing shape resonances, as, for example, the $He^-\ 1s2p^2\ ^4P$ state which is about 10 meV above the He $1s2p\ ^3P^o$ threshold [10].

That the possibilities (1) and (2) are realistic can be seen from calculations where the nuclear charge, Z, is larger than 2, i.e., when nuclear attraction is increased and small MCHF calculations of heavily mixed wave functions converge relatively easily. For example, when $Z=3$, state-specific expansions of about ten terms yield the first three MCHF state-specific roots. When these are allowed to interact in a nonorthonormal CI (NONCI), the energies prove to be stable. The second root is 4.96 eV above the first, and the third root is only 0.25 eV above the second. These compact wave functions of Li ^2D TES have the following constitutions:

$$\text{first root:}\quad 0.908\psi(2s2p^2)-0.285\psi[(2s2p)\,^3P^o\,3p]-0.160\psi(2s^23d)-0.159\psi[(2p^2)\,^3P\,3d]-0.149\psi(3s2p^2)+0.140\psi[(2s2p)\,^1P^o\,3p], \tag{3a}$$

$$\text{second root:}\quad 0.858\psi(2s^23d)+0.496\psi[(2p^2)\,^1S\,3d]-0.113\psi[(2s2p)\,^3P^o\,3p], \tag{3b}$$

$$\text{third root:}\quad 0.982\psi[(2s2p)\,^3P^o\,3p]+0.142\psi(2s2p^2)-0.083\psi(3s2p^2). \tag{3c}$$

We point out that these orbitals are assigned by the hydrogenic number n, since the nuclear attraction in the Li TES is sufficient to create the central field. It is seen that Rydberg-like configurations such as $\Psi(2s^23d)$, $\Psi[(2p^2)\,^1S\,3d]$, and $\Psi[(2s2p)\,^3P^o\,3p]$, which play a major role as correlation vectors in the first root, become dominant in the second and third roots. As Z is gradually reduced to the value $Z=2$, three things occur when MCHF calculations are carried out. The first is that the distance between the energies of the first two roots is narrowed, while Rydberg-like configurations contributing to a valid Ψ_0 become OCL. (On the other hand, for the third root convergence of a state-specific MCHF calculation becomes impossible. Instead, an alternative method is necessary, based on NONCI, see below.) The second is that the outer p orbitals in the second state cannot be labeled with hydrogenic n. The number of its nodes is different than $n-l-1$. The third is that the character of the first three roots, when they are established for $Z=2$ (see below), is different, but the constituent main configurations remain essentially the same.

III. THE CALCULATION OF Ψ_0 AND E_0 OF THE FIRST THREE ^2D TES OF He^-

The calculation of Ψ_0 and E_0 used as imput the heuristic analysis of Sec. II and the experience on the lowest ^2D He^- TES, results of which we have already published [1,4]. We aimed at identifying the three lowest ^2D triply excited resonance states. For the first two states, the normal state-specific procedure was followed, with the final solutions obtained from a NONCI [1,4,11]. For the third one, for which the MCHF equations could not be solved reliably, localization was established indirectly: We carried out a series of NONCI calculations of increasing size, using functions spaces from the first two roots. For the final 996-term NONCI, we established variationally that the third root goes through a local minimum.

A. First state: $2p\leftrightarrow p$ radial correlation and internal couplings

One of the conclusions from the recent work on the lowest ^2D TES of He^- [1] is that the configurational character has a dependence on the radial part of the p orbitals. Specifically, if the two p electrons are restricted to occupy the same radial function, $2p$, from a RHF calculation or from a MCHF calculation with main configurations $2s2p^2$, $(2s2p)\,^1P^o\,3p$, $2s3p^2$, $2s^23d$, and $3d(2p^2)\,^1D$, ^3P (Table II of [1]), the configuration $2s2p^2$ dominates. The corresponding coefficients are 0.880, -0.266, -0.234, -0.195, -0.127, and 0.111. All orbitals can be labeled by hydrogenic n and are relatively compact. The average values for the radii of the MCHF $2s$, $2p$, $3s$, $3p$, and $3d$ orbitals are $\langle r_{2s}\rangle = 3.73$ a.u., $\langle r_{2p}\rangle = 6.76$ a.u., $\langle r_{3s}\rangle = 6.82$ a.u., $\langle r_{3p}\rangle = 10.49$ a.u., and $\langle r_{3d}\rangle = 5.65$ a.u.

On the other hand, calculations also showed that if the two p electrons are allowed to occupy different orbitals, then the character of the state is best represented by $2s2pp$, signifying the importance of radial correlation, which is expressed mainly by $2p\leftrightarrow p$ [1].

We now comment on the relation of angular momentum coupling to such configurations and the connection between main configurations generated by single and double orbital replacements from $2s2p^2\,^2D$. This analysis is even more useful for the second root discussed below.

(i) When the three electrons are coupled as $(2s2p)\,^3P^0\,3p$, if this configuration is included in the MCHF calculation convergence fails. This is because He $(2s2p)\,^3P^0$ is an open channel and, evidently, during optimization the outer p orbital cannot satisfy the condition of a bound orbital. This is why the list of MCHF configurations does not include the $(2s2p)\,^3P^o\,3p$ coupling.

(ii) Table II of [1] does not include the $2s(2p3p)\,^1D$ coupling either, which is created from the $(2p^2)\,^1D \rightarrow 2p3p$ single orbital excitation. The explanation is that this configuration, which contains as a component the $(2s2p)\,^3P^o\,3p$ configuration of (i), (see below), is taken into account by the presence of the $2s2p^2$ and $2s3p^2\,^2D$ configurations. This can be seen from the relationship of configurations with the orbitals from the MCHF calculation to configurations with transformed orbitals: The $2s2p^2$ and $2s3p^2\,^2D$ configurations are represented by one determinant, with the p^2 electrons coupled to ^1D symmetry. When we took the $2s$, $2p$, and $3p$ orbitals from the above MCHF calculation for the first root and constructed a 2×2 MCHF calculation with $2s2p^2$ and $2s3p^2$ configurations, a converged solution with energy $-0.721\,047$ a.u. was obtained. Each determinant is invariant to orthogonal transformations. Let us consider the transformed orbitals $2p_t = a2p + b3p$ and $3p_t = -b2p + a3p$, with $m_l = 1$, $m_s = \pm 1/2$. The wave function now contains the configurations $2s2p_t^2$, $2s3p_t^2$, and $2s(2p_t3p_t)\;\,^1D$ and we demand that $2s3p_t^2$ is eliminated. This constraint relates the 2×2 mixing coefficients to the orbital coefficients a and b, and yields, in conjunction with $a^2+b^2=1$, the orbital mixing coefficients, $a=0.8706$ and

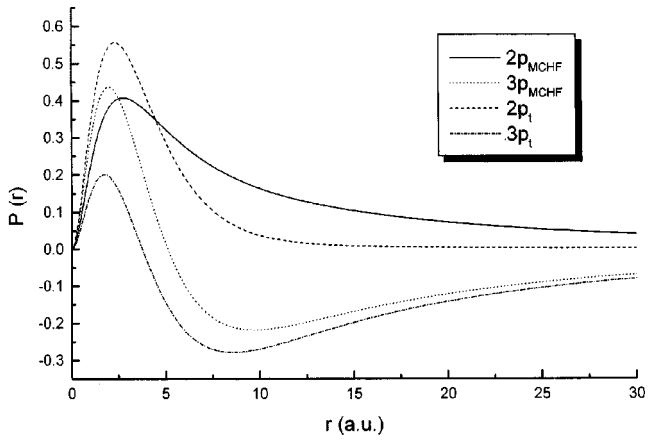

FIG. 1. Comparison of the canonical MCHF $2p$ and $3p$ orbitals with the $2p_t$ and $3p_t$ orbitals obtained via the transformation discussed in the text.

$b=0.4920$. The orbitals $2p_t$ and $3p_t$ are orthonormal. A 2×2 CI using the $2s2p_t^2$ and $2s(2p_t3p_t)\,^1D$ configurations yields the solution $\varepsilon(2\times2)=-0.721\,047$ a.u. As expected, this is the same energy as that obtained with the $2s2p^2$ and $2s3p^2$ configurations. The coefficients for the $2s2p_t^2$ and $2s(2p_t3p_t)\,^1D$ configurations are 0.648 and -0.761, respectively. This fact implies that, indeed, the $2p^2\leftrightarrow2pp$ radial correlation for the ^2D symmetry is very strong. Furthermore, it becomes even clearer that the two p electrons occupy different parts of space: The average values of r for the three orbitals are $\langle r_{2s}\rangle=3.73$ a.u., $\langle r_{2pt}\rangle=3.07$ a.u., and $\langle r_{3pt}\rangle=14.17$ a.u. and point to a situation of an inner p and an outer p electron. Figure 1 depicts the $2p_t$ and $3p_t$ together with the $2p$ and $3p$ orbitals from the MCHF calculation. (It is worth adding that the topology of two different p orbitals is confirmed by calculations of one- and two-electron radial densities using the fully correlated wave functions [12].)

The above 2×2 result has heuristic value and its essence remains when a large CI calculation is carried out. For example, a 117-term state-specific eigenvector, whose energy is $\varepsilon(117\times117)=-0.759\,280\,2$ a.u. (the accurate E_0 is $-0.760\,871\,4$ a.u.), produces the following coefficients for the three most significant configurations, $2s2p_t^2$, $2s(2p_t3p_t)\,^1D$, and $2s(2p_t3p_t)\,^3D$: 0.665, -0.612, and -0.268. Note the presence of the configuration with ^3D coupling, which is of course absent from the 2×2 CI, since the np^2 electrons couple only to a singlet D. The appearance of the triplet D coupling results from interactions in the energy matrix of higher order.

(iii) The fact that the MCHF solution with $2s3p^2$ contains, intrinsically, and in combination with the $2s2p^2\,^2D$ configuration, the contribution of the $2s(2p3p)\,^1D$ configuration implies that it contains contributions from the $(2s2p)\,^3P^o\,\varepsilon p$ continuum as well. This is because angular momentum coupling gives

$$2s(2p3p)\;^1D=\frac{\sqrt{3}}{2}(2s2p)\;^3P^o\,3p-\frac{1}{2}(2s2p)\;^1P^o\,3p \tag{4}$$

meaning that the $2s(2p3p)\,^1D$ configuration carries information from both the closed, $(2s2p)\,^1P^o$, and the open, $(2s2p)\,^3P^o$, channels.

We point out that a more direct indication of the significance of angular momentum coupling in open-shell structures for the quantitative understanding of the formation of resonance states was demonstrated by Komninos *et al.* [9], with the analysis and computation of the He^- $1s2s2p\;^2P^o$ resonance at 20.3 eV. There, a two-term MCHF wave function, $1s^22p+1s2s2p$, was shown to contain contributions from both the He $1s2s\;^3S$ open and the He $1s2s\;^1S$ closed channel, with respect to which the resonance can be labeled as *shape* or as *Feshbach*.

B. Second state: Orbital transformations and mixing of configurations

The construction and solution of MCHF equations for higher roots in calculations of multiply excited resonance states of ANIs is a rather complicated affair. The mixing of many configurations is strong, there are open channels, the binding potential is weak, and oscillations or divergences of the apparent solutions may occur. Nevertheless, our experience suggests that a reliable solution is possible for some cases. However, the interpretation of the character in terms of configurations may be vague if the direct MCHF solution is used, since some of the orbitals may loose the hydrogenic correspondence. In what follows we show how in the case of the second root, for which such difficulties exist, orbital transformations help clarify the interpretation of the electronic structure.

Starting from a 48-term expansion for the lowest ^2D He^- TES, state-specific convergence to a valid MCHF solution was achieved, keeping appropriate orbital orthogonality constraints. The MCHF energy is $-0.752\,227\,5$ a.u., which is just above that of the lowest TES. However, now the p orbitals do not have the hydrogenic correspondence. Instead, the calculation yields two orthonormal p orbitals, p_1 and p_2, that enter the main MCHF configurations, $2sp_1^2$, $2s^23d$, $(p_2^2)\,^3P\,3d$, $2sp_2^2$, and $(p_1p_2)\,^1D\;3s$, with coefficients 0.910, -0.239, -0.208, -0.159, and -0.102. The average values of the orbital radii are $\langle r\rangle_{2s}=3.856$ a.u., $\langle r\rangle_{p1}=4.520$ a.u., $\langle r\rangle_{3s}=5.877$ a.u., $\langle r\rangle_{p2}=6.285$ a.u., and $\langle r\rangle_{3d}=6.064$ a.u. One of the criteria of localization is the satisfaction of the virial theorem, which in this case gives 2.03.

Atomic correlated wave functions that do not consist of configurations with hydrogen-like central field orbitals do not allow the direct application of the usual qualitative language regarding electronic structure. Instead, interpretations can be achieved after the calculation of physically meaningful expectation values with the full wave functions [12]. Here, we show how the analysis that we gave for the first root can produce a picture of the basic structure of the second TES. In turn, this recognition supports the execution of large-scale calculations of its wave function, energy, width, and other properties.

Using the two configurations $2sp_1^2$ and $2sp_2^2$, we carry out a 2×2 careful MCHF optimization. The resulting energy for the second root is $-0.720\,004$ a.u. We then construct the

configurations $2s2p_t^2$ and $2s(2p_t3p_t)\,^1D$ using the same orbital transformation as before. The coefficients of this transformation are $a=0.446$ and $b=0.895$. The CI energy remains the same and the mixing coefficients of the new configurations are 0.729 and 0.685, respectively. The average values for the transformed orbitals are $\langle r_{2pt}\rangle = 2.77$ a.u. and $\langle r_{3pt}\rangle = 8.29$ a.u.

The picture that emerges is now clear. First of all, the transformed orbitals have hydrogen-like character and this is why we label them by a principal quantum number. Secondly, the two p electrons definitely reside in different parts of space, as a result of radial correlation. Thirdly, the second ^2D TES is a mixture of ''valence'' and ''Rydberg'' configurations, slightly tending toward the valence type. This picture did not change when we carried out an MCHF and a 117 $\times$117 CI with these orbitals. The main configurations and their coefficients are $c(2s2p_t^2)=0.7344$, $c[2s(2p_t3p_t)\,^1D]=0.5737$, $c[3d2p_t^2(^3P)]=-0.1918$, $c[3d2p_t^2(^1S)]=-0.0775$, $c(3s2p_t^2)=-0.0894$, $c(2s^23d)=-0.2286$, $c[3s(2p_t3p_t)\,^1D]=0.0585$, and $c(2s3d^2)=0.0513$.

Finally, another piece of information from the 2×2 CI results with the transformed orbitals which have heuristic value is the fact that the energies of the two roots lie very close to each other, the difference being only 28 meV. This fact suggests that if the addition of electron correlation does not destroy localization (it does not), there would be a good chance that a full computation would indeed uncover a new ^2D resonance state, with a major component reflecting the strong radial correlation in the lowest TES and lying only a few decades of meV above it.

We finally proceed with the systematic, large-scale calculations of the fully correlated wave function. Following the calculation of the zero-order 48-term MCHF wave function, the remaining localized correlation is added variationally in terms of separately optimized nonorthonormal function spaces. A 117-term expansion gave $-0.756\,6427$ a.u., with the virial being 2.030, a 359-term expansion gave $-0.758\,949\,1$ a.u., with the virial being 2.029, and a 778-term expansion gave $-0.759\,197\,3$ a.u., with the virial being 2.028.

The last step in the state-specific approach accounts for the residual interaction between the separately optimized first and second roots. The proximity to the first ^2D root, $E_0^{(1)}=-0.760\,871\,4$ a.u., of the above 778-expansion result for the second state ($\Delta E=46$ meV), implies that some root repulsion will occur. Indeed, a 996-term NONCI calculation produced the final, state-specific energies for the lowest two roots, before the interaction with the remaining part of the open channels, as follows:

$$E_0^{(1)}(\mathrm{NONCI})=-0.761\,990\,0 \text{ a.u.},$$

$$E_0^{(2)}(\mathrm{NONCI})=-0.757\,746\,9 \text{ a.u.}, \quad \Delta E=115 \text{ meV}. \quad (5)$$

C. Third state: An OCL wave packet, identified from the third root of NONCI calculations

As already mentioned, we could not obtain a valid MCHF solution for a third TES. Nevertheless, given the experimental observation and our results for the first two states, we decided to examine the possibility that such a TES can be identified from the convergence of NONCI calculations of increasing size, where the configurations are taken from the solutions for the first two roots. A small NONCI calculation that used 12 terms, six MCHF configurations from the lowest TES and six MCHF configurations from the second TES, gives for the first three roots: $E_1=-0.747\,601\,1$ a.u., $E_2=-0.727\,859\,8$ a.u., and $E_3=-0.617\,616$ a.u. Although, due to orbital overlaps, a direct recognition of the configurational character of the third root cannot be made, it becomes evident after renormalization that the OCL $2s^23d$ is the main dominant configuration. (See Sec. II for the Li case.) We then focused on the space of $2s^2d$ configurations. We constructed a 26×26 NONCI with dominant configurations and varied the radials of virtual orbitals of d symmetry. A local minimum was found at $E_3=-0.705\,676\,7$ a.u. for the root with a dominant $2s^2d$ configuration. The corresponding energies for the first two roots of this NONCI were $E_1=-0.747\,999\,0$ a.u. and $E_2=-0.729\,527\,6$ a.u., which are very close to the ones from the 12×12 NONCI. When a 718-term NONCI was carried out, the energies were $E_1=-0.761\,697\,2$ a.u., $E_2=-0.757\,406\,9$ a.u., and $E_3=-0.754\,348\,4$ a.u. It was evident that the third root closely approached the second one as a result of higher order interactions in the energy matrix. Finally, after intermediate trials, a 996-term NONCI, with the d space of virtual orbitals optimized variationally, converged to a local minimum for the third root (the virial is 2.04):

$$E_0^{(3)}(\mathrm{NONCI})=-0.756\,133\,7 \text{ a.u.} \quad (6)$$

The energy difference between $E_0^{(2)}$ (NONCI) and $E_0^{(3)}$ (NONCI) is 44 meV while $E_0^{(3)}$ (NONCI) is 58.431 eV above the He ground state. [$E(\mathrm{He})=-2.903\,724$ a.u., 1 a.u.(He) = 27.2077 eV.] These energy differences provide strong indication, before the calculation of the energy shifts and widths which are presented in the next section, that this solution can explain the experimentally observed third peak at 58.48 ± 0.02 eV. The formation of this OCL wave packet is due to strong electron correlations and channel couplings and its main contributors are configurations such as $2s^2d$, $(p^2)^1S\,3d$, $(2s2p)\,^1P^o\,p$ and $2sp^2$, where the orbitals p and d are virtual and do not have distinct hydrogenic features.

IV. ENERGY SHIFTS, TOTAL ENERGIES, PARTIAL AND TOTAL WIDTHS

As calculated, the NONCI wave functions include part of the coupling between open and closed channels, as well as mixing of the roots mediated by the open channels and indirect mixing of open channels through the resonances. The next phase in the overall calculation is the inclusion of the contribution to these states of the remaining part of the continuous spectrum, i.e., the part that causes delocalization and decay.

The calculation of the energy shifts and widths due to the various open channels was done as before [1,4]. Accordingly, by adopting the independent channel approximation, first the

TABLE I. Partial widths (γ_i) and total widths (Γ) in meV, of the second and third $He^-\ ^2D$ triply excited resonance states.

	γ_i	
Channel	Second	Third
$2s2p\ ^3P^0\ \varepsilon p$	0.0	7.1
$2s^2\varepsilon d$	0.8	41.8
$1s2s\ ^3S\ \varepsilon d$	1.1	3.8
$1s2s\ ^1S\ \varepsilon d$	0.6	0.5
$1s2p\ ^3P^0\ \varepsilon p$	1.0	0.8
$1s2p\ ^1P^0\ \varepsilon p$	0.3	0.2
This work	$\Gamma^{(2)}=\sum_i \gamma_i=4$	$\Gamma^{(3)}=\sum_i \gamma_i=54$
Expt. [2]	$\Gamma^{(2)}<2$	$\Gamma^{(3)}=70\pm 20$

partial shifts were obtained by solving self-consistently:

$$\mathcal{E}-E_0-\delta_i(\mathcal{E})=0, \tag{7a}$$

$$\delta_i(\mathcal{E})=\mathrm{P}\int_{E_i}\frac{|\langle\Psi_0|H-\mathcal{E}|U_i(\varepsilon)\rangle|^2}{\mathcal{E}-\varepsilon}d\varepsilon. \tag{7b}$$

P denotes principal value integration, ε is the energy variable, and E_i is the threshold energy for each channel. The $U_i(\varepsilon)$ are energy-normalized scattering wave functions whose scattering orbital is obtained numerically using a single- or a multiconfigurational [for He $(1s2s+1s^2)\ ^1S$ and for $(2s^2+2p^2)\ ^1S$] term-dependent core potential.

The total energy is obtained by adding to E_0 the sum of the partial shifts:

$$E=E_0+\Delta=E_0+\sum_i\ \delta_i. \tag{8}$$

Once the position of the resonance is determined, the partial widths are computed from

$$\gamma_i(E)=\frac{2\pi|\langle\Psi_0|H-E|U_i(E)\rangle|^2}{1-\delta_i'(E)}, \tag{9}$$

$\delta_i'(E)$ is the derivative at $\varepsilon=E$ of the energy shift at the position of the resonance state E. Its size signifies the degree of energy dependence of the width. For narrow resonances, $\delta_i'(E)$ is negligible and so the golden rule result is recovered.

Table I contains the partial and the total widths, $\Gamma^{(2)}$ and $\Gamma^{(3)}$, for the new TES, obtained using the Ψ_0 from the NONCI. The total width, $\Gamma^{(1)}=30$ meV, differs from the experimental value of 59 ± 4 meV [2] by a factor of 2. $\Gamma^{(2)}$ is narrow, about 4 meV, while $\Gamma^{(3)}$ is 54 meV. These two values verify the experimental observations, from which the widths were deduced to be <2 meV and 70 ± 20 meV, respectively [2]. We note that the calculation of $\Gamma^{(3)}$ showed that it is energy dependent. Specifically, the energy-dependence increased the magnitude of $\Gamma^{(3)}$ when compared with the value obtained from the energy-independent golden rule expression, i.e., without the contribution of $\delta_i'(E)$ in Eq. (9). (This value is 23 meV.)

As regards the calculation of the total shifts, the one for the first root is slightly different than the one reported in [1] where we used the Ψ_0 before the NONCI. The new $\Delta^{(1)}$ is 10 meV, compared with 19 meV given in [1]. The overall result is that the total energy produced by the present calculation is slightly lower.

The computed total shifts and total energies for the three resonances are

$$\begin{aligned}E^{(1)}&=E_0^{(1)}+\Delta^{(1)}=-0.761\,990+0.000\,369\ \text{a.u.}\\&=-0.767\,621\ \text{a.u.}\\&=58.282\ \text{eV above the He}\ ^1S\ \text{ground state,}\end{aligned} \tag{10a}$$

$$\begin{aligned}E^{(2)}&=E_0^{(2)}+\Delta^{(2)}=-0.757\,747+0.000\,924\ \text{a.u.}\\&=-0.756\,823\ \text{a.u.}\\&=58.412\ \text{eV above the He}\ ^1S\ \text{ground state,}\end{aligned} \tag{10b}$$

$$\begin{aligned}E^{(3)}&=E_0^{(3)}+\Delta^{(3)}=-0.756\,134+0.001\,305\ \text{a.u.}\\&=-0.754\,829\ \text{a.u.}\\&=58.466\ \text{eV above the He}\ ^1S\ \text{ground state.}\end{aligned} \tag{10c}$$

The experimental values of Gosselin and Marmet [2] are (58.283 ± 0.003) eV, (58.415 ± 0.005) eV, and (58.48 ± 0.02) eV, respectively.

V. SYNOPSIS

Structures in a variety of continuous spectra of atoms are normally associated with resonance (autoionizing) states. The fundamental reason for their formation is the capacity of the N-electron system to come into a nonstationary state whose wave function is temporarily $(t=0)$ localized in a local energy minimum inside the continuous spectrum. This possibility depends on the electronic structure and symmetry of the state and on the result of the competition between the corresponding attractive and repulsive forces. Thus, whereas the localized part of autoionizing states of neutral atoms and of positive ions is bound sufficiently strongly, the formation of resonance states in atomic negative ions, where the nuclear attraction on the outer electrons is weak, involves, in general, subtleties of interelectronic interactions. These facts have consequences as to the degree of difficulty and complexity of computation, as to the possibility of extracting pictures of electronic structure, and as to the efficiency of the existing theoretical approaches for identifying resonance states.

The theme of this paper was the prediction of the existence, from first principles, of unusual, multiply excited reso-

nance states of ANIs and the quantitative understanding of their electronic structure and their decay properties. The application involved three triply excited ^2D resonances of He^- around the He $2s2p\ ^3P^o$ threshold at 58.3 eV, and the results provided for the first time qualitative and quantitative interpretation of experimental results [2], whose explanation had remained a mystery for more than 12 years. The basic feature of the two new resonances is that they are caused by weakly bound wave packets whose main configurations appear as correlation vectors in the lowest intrashell state of the hydrogenic manifold $(n=2)$. Both the first and the second resonance states have considerable $2s2p^2$ character, with $2p^2 \leftrightarrow 2p\,p$ radial correlation. On the other hand, the third state is of the *open-channel-like* (OCL) type, where the wave packet contains a large component of $2s^2d$ configurations.

Finally, we add that the herein results can be tested by applying the complex coordinate rotation method (CCR) [13], paying attention to the choice of large expansions consisting of both orbital and r_{12}-dependent configurations. Such function spaces were found to be efficient for the previous CCR calculation of the low-lying TES of He^- [5].

ACKNOWLEDGMENT

We thank the Empirikion Foundation, Athens, Greece, for financial support to one of us (N.A.P.).

[1] C. A. Nicolaides and N. A. Piangos, Phys. Rev. A **64**, 052505 (2001).
[2] R. N. Gosselin and P. Marmet, Phys. Rev. A **41**, 1335 (1990).
[3] N. A. Piangos and C. A. Nicolaides, J. Phys. B **34**, L633 (2001).
[4] C. A. Nicolaides, N. A. Piangos, and Y. Komninos, Phys. Rev. A **48**, 3578 (1993).
[5] M. Bylicki and C. A. Nicolaides, Phys. Rev. A **51**, 204 (1995).
[6] S. J. Buckman and C. W. Clark, Rev. Mod. Phys. **66**, 539 (1994).
[7] S. Ormonde, F. Kets, and H. G. M. Heideman, Phys. Lett. **50A**, 147 (1974).
[8] P. J. M. van der Burgt, J van Eck, and H. G. M. Heideman, J. Phys. B **19**, 2015 (1986).
[9] Y. Komninos, G. Aspromallis, and C. A. Nicolaides, Phys. Rev. A **27**, 1865 (1983).
[10] C. A. Nicolaides, Y. Komninos, and D. R. Beck, Phys. Rev. A **24**, 1103 (1981).
[11] C. A. Nicolaides, Int. J. Quantum Chem. **60**, 119 (1996); **71**, 209 (1999).
[12] N. A. Piangos, Y. Komninos, and C. A. Nicolaides, One- and two-electron angular and radial densities of multiply excited resonances states of He^- (unpublished).
[13] G. D. Doolen, J. Phys. B **8**, 525 (1975); Int. J. Quantum Chem. **14**, 523 (1978).